Mechanism of Enolase: The Crystal Structure of Asymmetric Dimer Enolase−2-Phospho-D-glycerate/Enolase−Phosphoenolpyruvate at 2.0 Å Resolution[†,‡]

Erli Zhang,[§,||] John M. Brewer,[⊥] Wladek Minor,[▽] Lionel A. Carreira,[#] and Lukasz Lebioda*[,§]

Department of Chemistry and Biochemistry, University of South Carolina, Columbia, South Carolina 29208, Department of Biochemistry & Molecular Biology, University of Georgia, Athens, Georgia 30602, Department of Molecular Physiology and Biological Physics, University of Virginia, Charlottesville, Virginia 22901, and Department of Chemistry, University of Georgia, Athens, Georgia 30602

Received May 27, 1997; Revised Manuscript Received August 4, 1997[⊗]

ABSTRACT: Enolase, a glycolytic enzyme that catalyzes the dehydration of 2-phospho-D-glycerate (PGA) to form phosphoenolpyruvate (PEP), is a homodimer in all eukaryotes and many prokaryotes. Here, we report the crystal structure of a complex between yeast enolase and an equilibrium mixture of PGA and PEP. The structure has been refined using 29 854 reflections with an $F/\sigma(F)$ of ≥ 3 to an R of 0.137 with average deviations of bond lengths and bond angles from ideal values of 0.013 Å and 3.1°, respectively. In this structure, the dimer constitutes the crystallographic asymmetric unit. The two subunits are similar, and their superposition gives a rms distance between C_α atoms of 0.91 Å. The exceptions to this are the catalytic loop Val153−Phe169 where the atomic positions in the two subunits differ by up to 4 Å and the loop Ser250−Gln277, which follows the catalytic loop Val153−Phe169. In the first subunit, the imidazole side chain of His159 is in contact with the phosphate group of the substrate/product molecule; in the other it is separated by water molecules. A series of hydrogen bonds leading to a neighboring enolase dimer can be identified as being responsible for ordering and stabilization of the conformationally different subunits in the crystal lattice. The electron density present in the active site suggests that in the active site with the direct ligand−His159 hydrogen bond PGA is predominantly bound while in the active site where water molecules separate His159 from the ligand the binding of PEP dominates. The structure indicates that the water molecule hydrating carbon-3 of PEP in the PEP → PGA reaction is activated by the carboxylates of Glu168 and Glu211. The crystals are unique because they have resolved two intermediates on the opposite sides of the transition state.

Enolase (2-phospho-D-glycerate hydrolyase, EC 4.2.1.11) is a "metal-activated metalloenzyme" (Brewer, 1981) that catalyzes the dehydration of 2-phospho-D-glycerate (PGA)[1] to phosphoenolpyruvate (PEP) in the glycolytic pathway, and the reverse reaction, the hydration of PEP to PGA, in gluconeogenesis (Wold, 1971). The yeast enzyme (isozyme 1) is a dimer having two identical subunits (Brewer & Weber, 1968; Brewer et al., 1970) with a molecular mass of 46 691 Da as the apomonomer (Brewer, 1981; Chin et al., 1981; Wedekind et al., 1994). Enolase has an absolute requirement for certain divalent metal ions for activity. The natural cofactor is Mg^{2+}, which gives the highest activity (Wold & Ballou, 1957; Brewer, 1985). Two types of metal binding sites contribute to catalysis (Faller et al., 1977). Metal binding in site I, traditionally called "conformational", induces a conformational change in the active site and enables binding of substrate or substrate analogues (Brewer & Weber, 1966; Faller & Johnson, 1974). Following binding of a substrate or a substrate analogue, the second metal ion, called "catalytic", can bind in site II (Hanlon & Westhead, 1969; Brewer, 1971), and then the catalytic reaction occurs (Faller et al., 1977). While different metal ions will bind to a given site with different affinities, in the case of Mg^{2+} and the first row transition metal divalent cations, which produce enzymatic activity, metal ion binding in the catalytic site is weaker when compared with that in the conformational site (Faller et al., 1977; Brewer, 1985). The metal ion site nomenclature is derived from the macroscopic effects, including subunit association (Brewer & Weber, 1968), of metal ion binding at these sites, although it does not necessarily reflect the metal ion function at atomic resolution.

Initially, the crystal structure of yeast enolase was determined to be the apoenzyme (Lebioda et al., 1989) and was followed by studies of catalytic and inhibitory complexes carried out in several laboratories. The structure of the precatalytic complex, enolase with an equilibrium mixture of PGA/PEP and one Mg^{2+} ion, was initially determined using the tetragonal form of crystals grown in 2.2 M

[†] This work has been supported by the National Science Foundation (Grants MCB 9604004 and BIR 9419866) and DOE (Grant DE-FG-95TE00058).

[‡] The atomic coordinates for this complex of enolase have been deposited in the Brookhaven Protein Data Bank as entry 2one.

* Corresponding author. E-mail: lebioda@psc.sc.edu. Telephone: (803) 777-2140. Fax: (803) 777-9521.

[§] University of South Carolina.

[||] Present address Park-Davis Pharmaceutical Research, division of Warner-Lambert Company, Ann-Arbor, MI 48105-2430.

[⊥] Department of Biochemistry & Molecular Biology, University of Georgia.

[▽] University of Virginia.

[#] Department of Chemistry, University of Georgia.

[⊗] Abstract published in *Advance ACS Abstracts,* September 15, 1997.

[1] Abbreviations: EDTA, ethylenediaminetetraacetate; NMR, nuclear magnetic resonance; PEP, phosphoenolpyruvate; PGA, 2-phospho-D-glycerate; PEG, polyethylene glycol.

S0006-2960(97)01245-2 CCC: $14.00

ammonium sulfate at pH 5 (Lebioda & Stec, 1991). These investigations showed that the conformation of the glycerate part of the PGA molecule bound in the active site was planar, as opposed to the orthogonal one observed in the unbound state (Lis, 1985). The electron density of the ligand, however, was not good enough to establish if the conformational metal ion coordinates the substrate through the hydroxyl or carboxylate moiety. On the basis of data suggesting metal binding through the hydroxyl (Nowak et al., 1973; Anderson et al., 1984), the substrate was positioned accordingly. The other important observation was the fact that in the precatalytic complex the loops Ser36−His43, Val153−Phe169, and Asp255−Asn266 move up to 8 Å and approach the active site to assume the "closed" conformation as opposed to the "open" conformation found in the native enolase and some inhibitory complexes. The enzyme may also be crystallized at more alkaline pH values using PEG (Zhang et al., 1994; Larsen et al., 1996). This is helpful, as the pH optimum of the yeast enzyme is at 7.8 (Wold & Ballou, 1957), and the catalytic Mg^{2+} binding is much stronger at the more alkaline pH (Lebioda et al., 1989). Recently, Larsen et al. (1996) determined the structure of the catalytic complex of PEG-crystallized enolase at 1.8 Å resolution and obtained superb maps which allowed them to establish among other things that, contrary to the previously held view, the conformational metal ion (in site I) coordinates the substrate through its carboxylic group. In their crystal form, there is also a dimer per asymmetric unit but there are no significant differences between the subunits. Our serendipitous finding reported herein of the asymmetric complex of enolase with PGA and PEP ordered in the crystal lattice as well as the existence of intermediate conformational states between the closed and open states makes enolase catalysis among the best structurally characterized. The structures of apoenolase (Stec & Lebioda, 1991), enolase−Mg^{2+} (Wedekind et al., 1995), enolase−Mg^{2+}−PGA (this work), enolase−PGA−$2Mg^{2+}$ (Larsen et al., 1996), and enolase−Mg^{2+}−PGA/PEP (this work) are now available in addition to those of an array of inhibitory complexes. Here, we describe the asymmetric structure and discuss its contribution to our understanding of the catalytic mechanism of enolase. A preliminary account of some of these results has appeared in abstract form (Lebioda et al., 1996).

MATERIALS AND METHODS

Complex Formation and Crystal Data Collection. Crystals of yeast enolase suitable for X-ray diffraction studies were obtained as described previously (Zhang et al., 1994). Briefly, a drop containing equal volumes of enolase solution in water and 22% PEG 4000 in 100 mM Tris buffer (pH 9.3) and 200 mM Li_2SO_4 was equilibrated against PEG 4000. Crystals appeared within 10 days, and growth was complete within 3 weeks. The crystals were dropped into capillaries, which were filled with artificial mother liquor solution obtained by increasing the concentration of PEG 4000 to 25%. This solution was gradually replaced using the gradient diffusion method (Lebioda & Zhang, 1992) with a solution of 25% PEG 4000, 200 mM ammonium sulfate, 10 mM Mg^{2+}, and 5 mM 2-phospho-D-glycerate in 100 mM Tris-HCl buffer at pH 9.3. The crystals were monoclinic, space group $P2_1$, with the following unit cell dimensions: a = 63.06 Å, b = 110.22 Å, c = 66.20 Å, and β = 112.7°. The data were collected with a Rigaku R-AXIS II system equipped with a graphite monochromator and processed with HKL software (Otwinowski & Minor, 1997).

A total of 96 445 observations with an F^2 of $\geq 1\sigma(F^2)$ was merged and averaged, yielding 30 646 symmetry-independent reflections with an R-merge of 5.6%. The reflections constituted 83.3% of all possible reflections to 2.00 Å resolution. The structure refinement employed 29 854 reflections with a resolution of better than 9 Å.

Structure Solution and Refinement. The structure of the precatalytic ternary complex enolase−Mg^{2+}−PGA was solved by molecular replacement with the AMORE program of Navaza (1987, 1990), using the coordinates of the same complex determined at 2.2 Å resolution in the tetragonal crystal form at high salt concentrations (Lebioda & Stec, 1991). A single subunit was used as the search model. A cross-rotation function, calculated from the data in a 4−8 Å resolution range, showed two prominent peaks with heights of 11.2σ and 10.8σ, related by 180°. Translational searches gave solutions for both rotational peaks. One of the solutions was fixed, and the search for the other translational solution was repeated. Then, the second position was fixed and the position of the first solution optimized. The model was refined as two rigid bodies and gave an R of 34.1%. The two subunits were displayed, and the correct asymmetric dimer was selected. The model was further refined using the simulated annealing and temperature factor refinement with the program XPLOR (Brunger, 1992) using the data in a 7−2.8 Å resolution range. It gave an R of 19.3% without waters and ligands. Further refinement was carried out by restrained least-squares fitting (Hendrickson & Konnert, 1980) with the PROFFT program (Finzel, 1990) with the maximum value of the B-factors being limited to 50 Å^2. The model was inspected and manually rebuilt several times. The ligands were added to fit omit Fourier maps. The refinement converged at an R of 13.7%; the rms deviations from the target geometries were 0.014 Å for the bond length, 3.1° for bond angles, and 0.033 Å from planarity. A plot of average isotropic temperature factors as a function of residue number is represented in Figure 1.

Calculations of pK_a values were performed using the SPARC program (Hilal et al., 1994).

RESULTS

Model Quality. The electron density is very good except for the region of residues 265−271, which in both subunits has relatively poor density. In this region, the peptide chain can be followed but its conformation is not apparent. Also, the density of residues 30−40 in subunit B is not clear and indicates some disorder. Outside these regions, all residues in each subunit have well-defined side chains except some surface residues (almost all lysines) listed in Table 1. The electron density at His159 in subunit B, which is extensively discussed below, is shown in Figure 2. The refined structure is very similar to those determined previously for yeast enolase, and the hydrogen bonding pattern is also very similar to those reported previously (Stec & Lebioda, 1990; Larsen et al., 1996).

Subunits. The α-carbons of the two subunits superimpose with a rms displacement of 0.91 Å. There are two loops, discussed below, on which the relative displacements reach over 4 Å. When these loops are excluded from the comparison, the two subunits superimpose with a rms

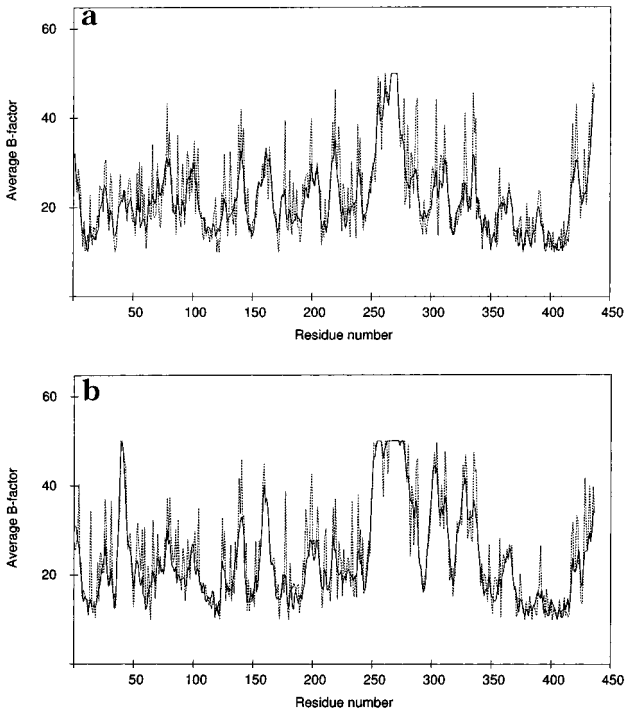

FIGURE 1: Average temperature factor as a function of residue number (a) for subunit A, in the closed conformation, and (b) for subunit B, in the loose conformation. The dotted lines are the average temperature factors of the side chain atoms.

displacement of 0.41 Å. One of the loops is the catalytic loop Val153−Phe169. In subunit A, the imidazole of His159 is in direct contact with the phosphate of the substrate and the loop conformation is very similar to that reported by Larsen et al. (1996), so it will be referred to as the closed conformation. In subunit B, there are water molecules separating the side chain of His159 from the phosphate and the relative position of the tip of the loop is different by about 3.5 Å from that in subunit A. A superposition of these loops obtained by least-squares fitting of the conformationally invariant parts of the subunits is shown in Figure 3. A series of interactions connects the subunits to the neighboring enolase dimer and stabilizes this loop conformation (Figure 4). It will be referred to as the "loose" conformation to differentiate it from the open conformation found in the native enolase molecule (Stec & Lebioda, 1990) and in some inhibitory complexes (Brewer & Lebioda, 1997). The positions of C_α in the Asn155−Gln167 region differ in the two subunits from 1 to 5 Å. The second loop that deviates significantly from the 2-fold symmetry is the loop Ser250−Gln277 where the positions of C_α also differ from 1 to 5 Å. This loop is in contact with the catalytic loop Val153−Phe169 and follows the catalytic loop toward the active site (Figure 5). Its sequence is fairly conserved among animal enolases, but in plant enolases, the loop is longer by two residues and in bacterial enolases shorter by four [for a recent alignment of enolase sequences, see Brewer and Lebioda (1997)]. One may speculate that its role is related to the observed asymmetry and perhaps protein dynamics.

Table 1: Disordered Side Chains, with an Electron Density of $<1.0\sigma$

amino acid of subunit A	disordered atoms	amino acid of subunit B	disordered atoms
Lys53	ξ	Lys4	δ, ϵ, ξ
Lys66	ϵ, ξ	Ser37	β, γ
Lys78	δ, ϵ, ξ	Lys53	$\gamma, \delta, \epsilon, \xi$
Lys104	ξ	Lys59	ϵ, ξ
Lys131	δ, ϵ, ξ	Lys78	ξ
Lys177	δ, ϵ, ξ	Lys138	δ, ϵ, ξ
Lys199	$\gamma, \delta, \epsilon, \xi$	Lys140	$\gamma, \delta, \epsilon, \xi$
Lys257	δ, ϵ, ξ	Lys194	ξ
Asp261	β, γ, δ	Lys198	ϵ, ξ
Lys336	$\gamma, \delta, \epsilon, \xi$	Lys254	ϵ, ξ
Lys337	ϵ, ξ	Lys257	$\gamma, \delta, \epsilon, \xi$
Lys435	$\gamma, \delta, \epsilon, \xi$	Lys287	δ, ϵ, ξ
		Lys336	δ, ϵ, ξ
		Lys435	$\gamma, \delta, \epsilon, \xi$

The least-squares superpositions of subunit A on subunits A and B of the catalytic complex of Larsen et al. (1996) gave rms values of 0.46 and 0.43 Å and 0.36 and 0.33 Å, respectively, when the 254−272 region was omitted from the calculations. These values are not far from the rms displacement of 0.27 Å obtained in the self-rotation of subunits of the catalytic complex (Larsen et al., 1996). As

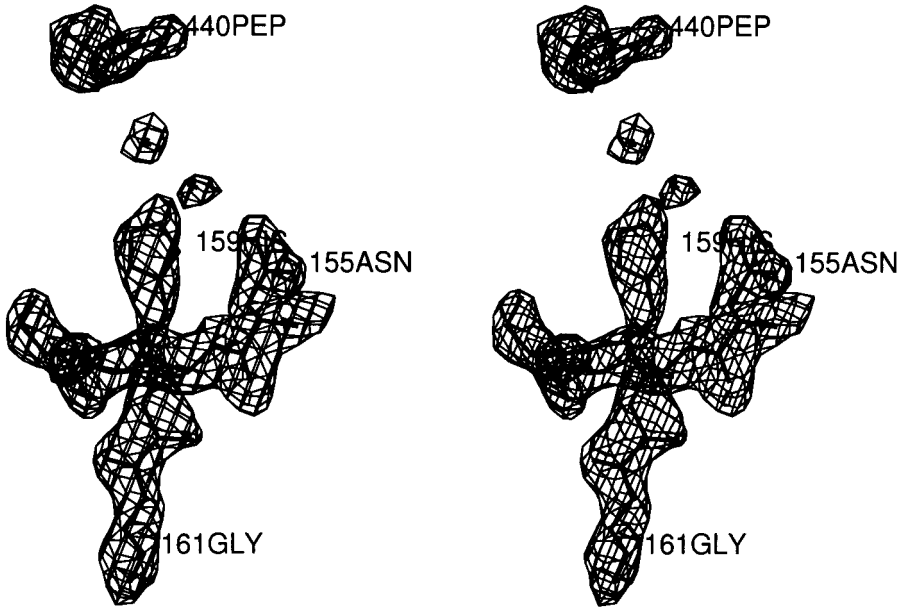

FIGURE 2: Electron density for the loop 155−161 in the loose conformation in subunit B. The $2|F_o| - |F_c|$ map is contoured at the 1.1σ level.

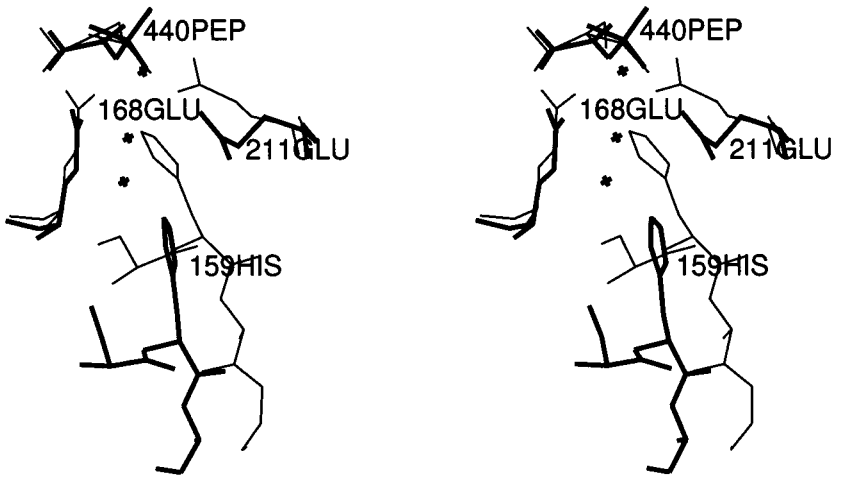

FIGURE 3: Active sites of subunit A and subunit B superimposed. Subunit A in the closed conformation is shown with the thin line, while subunit B in the loose conformation is shown with the bold line.

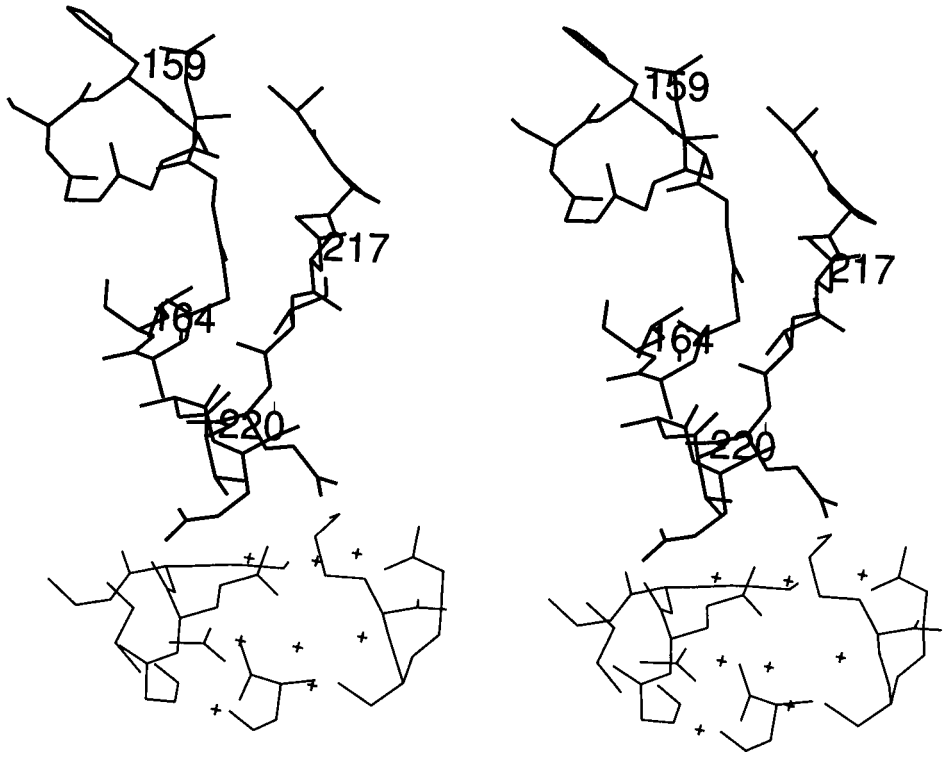

FIGURE 4: The loose conformation of the loop 155−164 in subunit B (in bold) is stabilized by interactions with residues 217−220 (in bold) from the same subunit which in turn interact with residues 120−126 and 82−85 of a neighboring dimer (the thin line).

expected, subunit B compares to the catalytic complex of Larsen et al. (1996) in a manner similar to that of subunit A; the rms displacements for the two subunits are 0.99 and 0.95 Å, respectively.

Active Sites. The position of the loop Val153−Phe169 is correlated with the ligand electron density. In subunit A, the density corresponds very well to that expected for the PGA ligand as there is a lobe for the hydroxyl moiety (Figure 6) and is similar to that observed in the catalytic complex (Larsen et al., 1996). In contrast, in subunit B, there is no density for the hydroxyl moiety but there is a density peak which can be attributed to a water molecule located between the side chains of Glu168 and Glu211 and positioned for nucleophilic attack on carbon-3 (Figure 7). The position of this water molecule could not be located in the catalytic complex of Larsen et al. (1996) in which only PGA is present in both subunits (see below). Thus, the structure of subunit A images the precatalytic complex in the PGA dehydration reaction, while subunit B images the precatalytic complex in the hydration of PEP. Below, we will refer to subunit A as the PGA subunit and to subunit B as the PEP subunit.

In the PGA subunit, the electron density in the catalytic metal binding site is weak though clearly visible (not shown). We believe that this indicates the presence of Li^+ there rather than a partial occupancy of Mg^{2+} since the concentration of magnesium ion (∼10 mM) was sufficient to ensure binding in the absence of a competing ligand. Lithium ion was present in the mother liquor at 400 mM, and it is likely that the gradient soaking procedure has not washed it out completely. In the refinement, its temperature factor converged at 16 $Å^2$, which is close to the values of 26 and 25 $Å^2$ obtained for the Mg^{2+} ions. Lithium ions inhibit enolase (Kornblatt & Musil, 1990); thus, the subunit represents not the catalytic but an inhibitory complex, though Kornblatt and

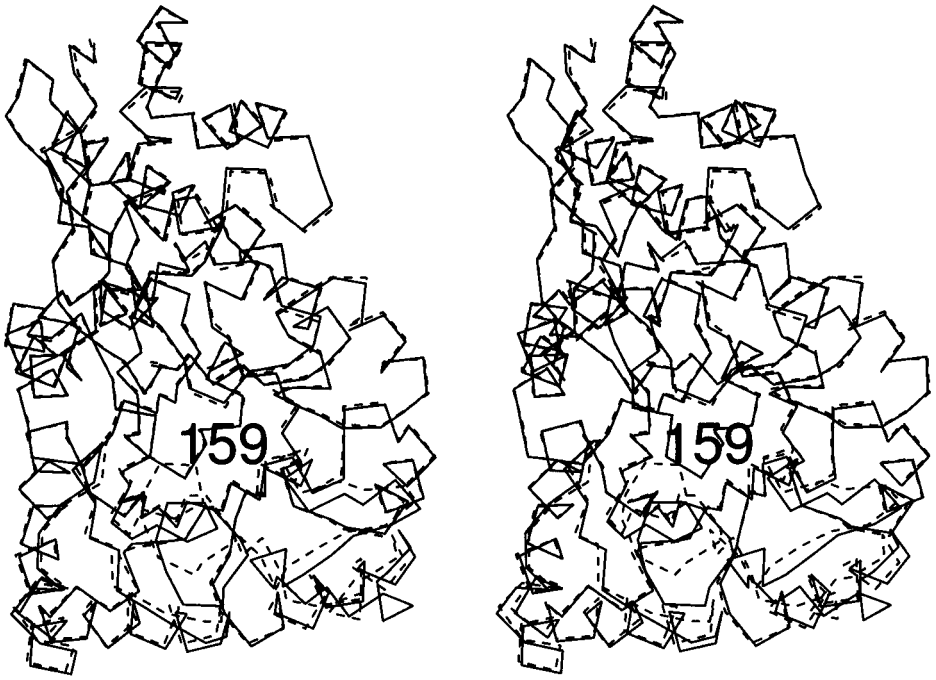

FIGURE 5: Least-squares superposition of C_α plots for subunit A in the closed conformation (broken line) and subunit B in the loose conformation (solid line).

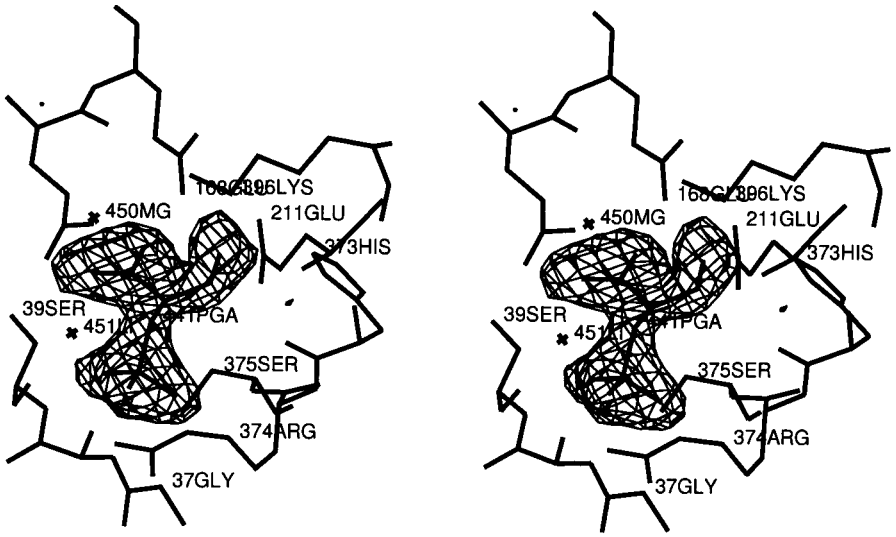

FIGURE 6: Substrate molecule, 2-phospho-D-glycerate, bound in the active site of subunit A. The electron density is from an omit, $||F_o| - |F_c||$, map contoured at the 3σ level.

Musil (1990) presented evidence suggesting Li^+ could produce some level of activity if it binds in the catalytic site [cf. Brewer and Collins (1980)]. In standard assay medium (Westhead, 1966) [0.05 ionic strength Tris-HCl (pH 7.8), 1 mM $MgCl_2$, and 1 mM PGA)] containing 25% PEG 4000 and 200 mM Li_2SO_4, the activity of the enzyme is 0.014% of the value in the absence of PEG and lithium sulfate.

The position of the ligand in the active site of the PGA subunit and most of the interactions between substrate/product molecules agree very well with those reported by Larsen et al. (1996) for the catalytic complex. An exception to this is the environment of the PGA hydroxyl which makes a close contact, 2.4 Å, not only with the O_ϵ of Glu211 but also with the O_ϵ of Glu168 at a distance of 2.3 Å. Such short distances are indicative of the existence of two strong hydrogen bonds (Jeffrey & Saenger, 1991). One of the hydrogen atoms forming these bonds comes from the hydroxyl, and the other must originate from one of the carboxylic acids; i.e., their proximity suggests Glu168 and Glu211 share a proton (Brewer et al., 1997). It has been shown that the mutation of either Glu168 or Glu211 to glutamate in yeast enolase reduces its activity by a factor of at least 10^{-4} (Brewer et al., 1993; Sangadala et al., 1995; Poyner et al., 1996). The enolase reaction shifts the proton from the donor, carboxylic acid, to the acceptor, hydroxyl, with the formation of a water molecule. The stronger the hydrogen bond, the more symmetric the potential energy well and the less activation energy is required for the proton shift. Since hydrogen bonding is cooperative, i.e., hydrogen bond donors are better hydrogen bond acceptors (Jeffrey & Saenger, 1991), the elimination of the carboxylic acid/carboxylate groups of either Glu168 or Glu211 by the mutations replaces the system $COO{-}H{\cdots}O{-}H{\cdots}{}^{-}OOC$ having strong hydrogen bonds present in the wild type enolase with the system $HNH{\cdots}O{-}H{\cdots}{}^{-}OOC$ in which there is no acidic proton capable of strong hydrogen bond

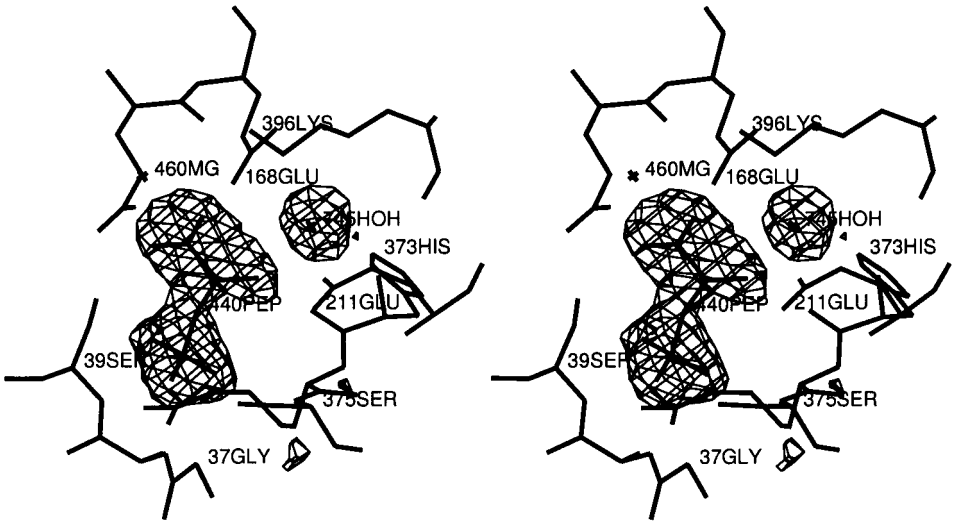

FIGURE 7: Substrate molecule, phosphoenolpyruvate, bound in the active site of subunit B. The electron density is from an omit, $||F_o| - |F_c||$, map contoured at the 3σ level.

formation and hence with very low potential for the proton transfer to the hydroxyl group.

Since the geometry of the catalytic complex has been discussed extensively by Larsen et al. (1996), we analyze below only those features of the PGA subunit that are important for the subsequent discussion of the PEP subunit. Below, the average distances determined in the catalytic complex by Larsen et al. (1996) are given in parentheses. The N_ξ atom of Lys345 forms a hydrogen bond to a water molecule at a distance of 2.7 Å (2.8 Å) and a bifurcated hydrogen bond to the oxygen atoms of the carboxylate of Asp320 at distances of 2.8 and 2.8 Å (3.0 and 2.9 Å). Its other important neighbors are carbon-2 of PGA at a distance of 3.5 Å (3.1 Å), C_ξ and N_ϵ of Arg374 at 4.0 and 3.9 Å (3.9 and 3.7 Å), and an oxygen atom of the phosphate group at 3.6 Å (3.6 Å). The geometry of hydrogen bonds is such that the third, potential hydrogen bonding direction of the N_ξ atom of Lys345 is in the general direction of carbon-2 of the PGA molecule. The distance between the N_ϵ atom of His159 and the closest O atom of the phosphate group is 3.2 Å (3.1 Å).

In the PEP subunit, the partial disorder of Ser39 did not allow us to evaluate the presence of Li^+ in the catalytic metal binding site. The most important feature, the catalytic water molecule, 745O in Figure 7, has four neighbors in an approximately tetrahedral arrangement: O_ϵ of Glu168 at 3.0 Å, O_ϵ of Glu211 at 2.7 Å, N_ϵ of His373 at 2.6 Å, and carbon-3 of the PEP at 3.1 Å. The angle O−C3−C2 is 117°, and the torsion angle O−C3−C2−C1 is 71°, indicating that the nucleophilic attack takes place approximately in the plane bisecting the H−C−H angle and at an angle close to 107° as predicted by Burgi et al. (1974). The environment of Lys345 is significantly different from that in the PGA subunit. The N_ξ atom also forms the bifurcated hydrogen bond with the oxygen atoms of the carboxylate of Asp320 at distances of 3.0 and 2.7 Å; however, there is no water molecule in the vicinity, and the second hydrogen bond is to an oxygen atom of the phosphate moiety at a distance of 2.9 Å. The distance to carbon-2, 3.5 Å, is the same as that in the PGA subunit, but the distances to the C_ξ and N_ϵ atoms of Arg374 are longer (4.4 and 4.2 Å, respectively). His159 does not have a contact with the PEP molecule; the shortest distance, between a N atom and an O atom of the phosphate, is 6.4 Å. Two water molecules at hydrogen bonding distances of 3.0 and 3.3 Å fill the space at the phosphate group (Figure 8).

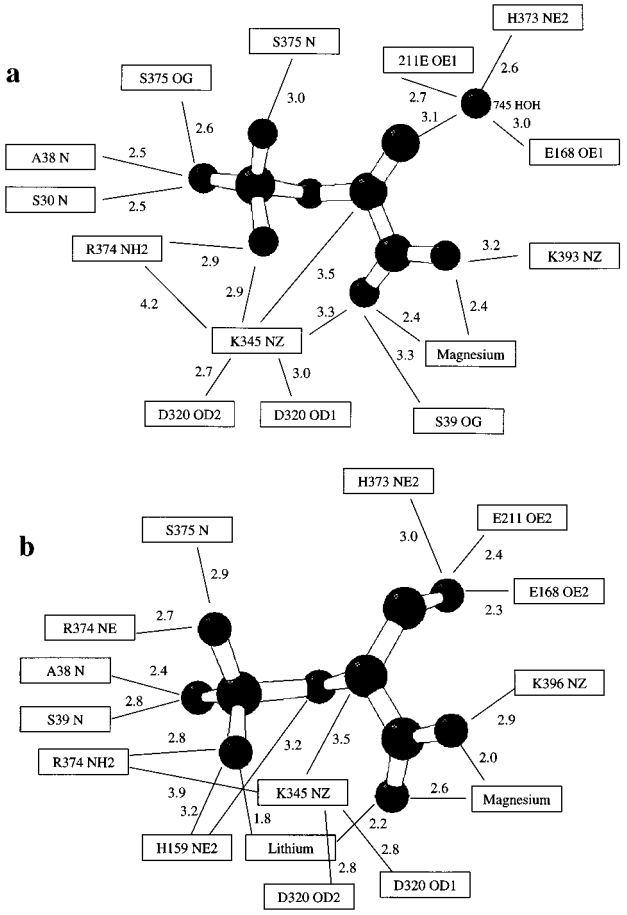

FIGURE 8: Environment of (a) the PEP molecule and (b) the PGA molecule in the active site of enolase. The distances are in angstroms.

DISCUSSION

Asymmetry of homooligomeric proteins can seldom be detected using X-ray crystallography because of the averaging effect of the crystals. To resolve the asymmetry, the crystal-packing forces must be selective and stabilize the

asymmetric oligomers; if subunits crystallize randomly in alternate conformations, the process results in disorder. A convincing resolution of asymmetric dimers was observed in α-chymotrypsin (Tulinsky & Blevins, 1987), for which anticooperativity of the subunits is well-documented. However, for enolase, there has been no evidence of subunits working in a correlated manner. Yeast enolase monomers dissociated at 40 °C are active in the presence of Mg^{2+} and substrate/product (Holleman, 1973). The ordering of ligands found in the subunits must be explained by fortuitous stabilization by crystal packing forces of the closed conformation in one site and the loose conformation in the other site and a correlation of the conformation with the ligand affinity. Indeed, if cooperativity or anticooperativity was an intrinsic property of the enolase dimer, the structure of the catalytic complex (Larsen et al., 1996) would show disorder between the closed and loose conformations, while such disorder positively is not observed. It rather appears that the crystal-packing forces in the crystal form studied by Larsen et al. (1996) stabilize the closed conformation. Such a hypothesis finds support in the superb fit of their electron density to the PGA molecule, including the pyramidal geometry at carbon-2 [see Figure 3 and Figure 5 in Larsen et al. (1996)]. If a significant amount of PEP were present, the disorder would likely distort the density. At enolase equilibrium at room temperature, it is expected that the ratio of PGA:PEP bound in the active site is 1:1 (Brewer & Ellis, 1983; Burbaum & Knowles, 1989). However, the data of Larsen et al. (1996) were obtained at −160 °C, and this may be a factor.

The catalytic activity of enolase usually has been analyzed in the glycolytic direction, dehydration of PGA. At the pH optimum of the enzyme, the rate-limiting step is the breakage of the carbon-2 hydrogen covalent bond (Shen & Westhead, 1973), though the loss of OH^- is a "kinetically significant" step (Anderson et al., 1994). Thus, the central problem in enolase catalysis is how a relatively nonacidic hydrogen atom is removed from the substrate, that is what factors influence the pK_a of the proton on carbon-2 and where the proton is transferred. Calculations (Hilal et al., 1995) suggest that a rotation of the carboxylate of the substrate around the carbon-1−carbon-2 bond by 90°, so that its oxygen atoms lie in the plane formed by three carbon atoms (the "planar" conformation), lowers the pK_a of the proton on carbon-2 in trianionic PGA from 58.3 to 16.5. Neutralization of the charge on the carboxylate and a change of the net charge on the phosphate of PGA from −2 to +1 yield a pK_a of 9.0. The different positioning of the substrate and placement of the metal ions, to reflect the geometry observed by Larsen et al. (1996) and in this report, make little difference to this value. The conformation of PGA, which is not far from the planar, is stabilized by interactions of the oxygen atoms of its carboxylate with the N_ϵ of Gln167 at 2.7 Å and N_ξ of Lys396 at 2.9 Å and the metal ions. The environment of the PGA trianion balances its charges; two Mg^{2+} ions, His159, Arg374, Lys396, and the proton at the hydroxyl all work to withdraw electrons from carbon-2.

His159, proposed as the catalytic base by Duquerroy et al. (1995), is at the other side of the PGA molecule and cannot abstract the proton from carbon-2 in the PGA dehydration reaction. Lys345 was proposed to function in this role (Wedekind et al., 1994; Larsen et al., 1996; Reed et al., 1996) as in the vicinity there is no other residue from the enzyme capable of acting as an acid/base. The only concern about its role is the close contact with Asp320 that could excessively stabilize the positive charge on N_ξ. The mutants of Lys345 have little activity (Wedekind et al., 1996; J. M. Brewer et al., in preparation), less than 0.01% for Lys345Ala or -Met, but one can envision an alternative mechanism in which Lys345 rather than pulling the proton from carbon-2 pushes it toward the phosphate moiety, the only other possible acceptor of the proton. However, calculations indicate that the major factor affecting the pK_a of the amino group of Lys345 is the electrostatic field of Arg374. When the separation between Lys345 and Arg374 is 4 Å, the calculated pK_a of the ϵ-ammonio is 7.8. Hence, Lys345 may indeed serve as the catalytic base despite its intrinsically high pK_a. Even more convincingly, it may be argued that the different environment of the Lys345 N_ξ atom in the PEP subunit reflects its different ionization state as the contacts with two anions, Asp320 and the phosphate, almost certainly ensure its protonation. Indeed, in the reverse reaction the hydration of the PEP ion, Lys345, is expected to deliver the proton.

The other major difference between the PGA and PEP complexes, the interaction between His159 and the phosphate, indicates that the position of the imidazol(ium) of His159 is correlated with the position and also, likely, the protonation state of Lys345. Two mechanistic scenarios can be envisioned. In the first, catalytic metal ion binding and the presence of the imidazolium of His159 at the phosphate can cause the ϵ-ammonio of Lys345 to move away from the phosphate, donate its proton somewhere, perhaps to the neighboring water molecule, and move toward carbon-2 of PGA. This movement would also be toward Arg374 and would be facilitated by interaction between the now electron rich ϵ-amino and the positive charge of the guanidinium. Such movement does not encounter any steric hindrance and would involve a small change in χ_1 or χ_3. Upon approach of the ϵ-amino to carbon-2, the abstraction of its proton would take place. We suggest that a crucial event preceding the proton abstraction from carbon-2 is the transfer of a proton from the imidazolium of His159 to the phosphate moiety, which affords additional electron withdrawing from carbon-2. Evidence for phosphate protonation during enolase turnover comes from the large shift observed in the ^{31}P NMR spectrum of substrate and product bound to yeast enolase observed by Brewer and Ellis (1983) which cannot otherwise be explained without a large change in the R−O−P bond angle, which is not observed. Further evidence can come from studies of mutants with His159 replaced by Gln and Glu. If indeed there is a proton transfer, the His159Glu mutant should have significant activity at acidic pH while the Gln mutant should be inactive. In an alternate scenario, the proton can be transferred from the ϵ-ammonio of Lys345 to the phosphate, perhaps after the dissociation of the catalytic metal ion, and eventually to the imidazole of His159.

In the reverse (hydration of PEP) reaction, the limiting step may be the nucleophilic attack of the hydroxide on carbon-3 of PEP which, like the forward reaction, would be facilitated by electron withdrawing from carbon-2. Site-directed mutants of His373 have been discussed in this connection (Brewer et al., 1997). Also, Lys345 must donate a proton to carbon-2 of PEP so it must be protonated. Such a state in the precatalytic complex is consistent with its

environment in the PGA subunit, further from Arg374 and closer to two anionic groups. Thus, the absence of His159 at the phosphate is the event controlling the Lys345 position and protonation.

In general, the results of work on yeast enolase have been highly reproducible and controversies correspondingly few. Those that have arisen recently stem from three factors: (1) the use of ammonium sulfate at relatively low pH (5−6) (Lebioda et al., 1989) to obtain the original crystals ("high-salt" crystals), (2) the PGA/PEP averaging in the structure of Lebioda and Stec (1991), which led to positioning the PGA 3-hydroxyl to coordinate with the conformational metal ion, and (3) the closeness of two charged residues, Asp320 and Arg374, to Lys345. The high-salt crystals have provided atomic coordinates (Lebioda et al., 1989) which have been repeatedly confirmed in different crystal forms (Wedekind et al., 1994; Larsen et al., 1996; this work), so the crystallization conditions do not significantly affect the overall conformation of the protein. They do appear to affect the position of the catalytic metal ion (at least in experiments with transition metals), which binds ca. 4 Å farther away from the conformational metal ion at lower pH values than it does at pH 7.8 (Zhang et al., 1994b; Lee & Nowak, 1992). Those conditions may also affect substrate binding, as there is unequivocal evidence for PGA 3-hydroxyl binding to conformational Ca^{2+} (which does not provide enzymatic activity) in high-salt crystals (Lebioda et al., 1991), and additional evidence that substrate or analogues may bind in two different orientations [reviewed in Brewer and Lebioda (1997)]. The relation of these observations to enzymatic activity is difficult to define precisely, as a small percentage of substrate bound in a different orientation may be undetectable in the X-ray structure but contribute strongly to the enzymatic activity observed under those conditions. The unexpected effect of the proximity of Arg374, in contrast to the minimal effect of Asp320, on the pK_a of the ϵ-ammonio of Lys345 resolves the last obstacle to reconciliation of the mechanistic proposals of the two groups.

We therefore suggest that, at pH 7.8, the mechanism is as follows. When PGA binds, its carboxyl is rotated through interactions with Gln167, Lys396, and both Mg^{2+} (Lebioda & Stec, 1991; Wedekind et al., 1994) and neutralized. Loop Ser36−His43 moves (Lebioda & Stec, 1991; Wedekind et al., 1994; Larsen et al., 1996) so the backbone carbonyl and side chain hydroxyl of Ser39 coordinate catalytic Mg^{2+} (Wedekind et al., 1994). Loops Val153−Phe169 and Ser250−Glu277 move together so His159 donates a proton to the phosphoryl of PGA (Brewer & Ellis, 1983). Thus, the negative charge on the phosphoryl is overneutralized through interaction with Arg374 and catalytic Mg^{2+}. This lowers the carbon-2 pK_a of PGA into the physiological range (Hilal et al., 1995). Lys345 moves closer to Arg374 which lowers the pK_a of its ϵ-ammonio group and leads to a loss of its proton so it can accept one from carbon-2 of PGA. The proton shared by Glu168 and Glu211 and forming a hydrogen bond to the PGA hydroxyl jumps from the carboxylate to the hydroxyl, making H_2O and PEP (Brewer et al., 1997). The readiness of the substituent on carbon-3 of PGA analogues to accept a proton is connected to the rate of the overall enzymatic reaction (Stubbe & Abeles, 1980; Brewer, 1985). In the reverse reaction, the hydration of PEP, the water held by Glu168, Glu211, and His373 (Lebioda & Stec, 1991) is deprotonated by one of the carboxylates and the generated OH^- adds to carbon-3, while a proton from the ϵ-ammonio group of Lys345 adds to carbon-2, thus eliminating the double bond between carbon-2 and carbon-3. His159 is not at the phosphoryl as the electron withdrawing from carbon-2 would be counterproductive to its protonation. While this is a complicated mechanism with a significant role left for protein dynamics, we feel that this description, based on the work of many groups, explains well the existing data and may serve as a basis for further experimentation.

ACKNOWLEDGMENT

We are grateful to Dr. G. H. Reed of the University of Wisconsin, Madison, for the early release of the coordinates of the catalytic complex.

REFERENCES

Anderson, S. R., Anderson, V. E., & Knowles, J. R. (1994) *Biochemistry 33*, 10545−10555.
Anderson, V. E., Weiss, P. M., & Cleland, W. W. (1984) *Biochemistry 23*, 2779−2786.
Brewer, J. M. (1971) *Biochim. Biophys. Acta 250*, 251−257.
Brewer, J. M. (1981) *CRC Crit. Rev. Biochem. 11*, 209−254.
Brewer, J. M. (1985) *FEBS Lett. 182*, 8−14.
Brewer, J. M., & Weber, G. (1966) *J. Biol. Chem. 241*, 2550−2557.
Brewer, J. M., & Weber, G. (1968) *Proc. Natl. Acad. Sci. U.S.A. 59*, 216−223.
Brewer, J. M., & Collins, K. M. (1980) *J. Inorg. Biochem. 13*, 151−164.
Brewer, J. M., & Ellis, P. D. (1983) *J. Inorg. Biochem. 18*, 71−81.
Brewer, J. M., & Lebioda, L. (1997) *Adv. Biophys. Chem. 6*, 111−141.
Brewer, J. M., Robson, R. L., Glover, C. V. C., Holland, M. J., & Lebioda, L. (1993) *Proteins 17*, 426−434.
Brewer, J. M., Glover, C. V. C., Holland, M. J., & Lebioda, L. (1997) *Biochim. Biophys. Acta 1340*, 88−96.
Brünger, A. T. (1992) *X-PLOR Version 3.1*, Yale University Press, New Haven, CT.
Burbaum, J. J., & Knowles, J. R. (1989) *Biochemistry 28*, 9306−9317.
Burgi, H. B., Dunitz, J. D., Lehn, J. M., & Wipf, G. (1974) *Tetrahedron 30*, 1563−1572.
Chin, C. C. Q., Brewer, J. M., & Wold, F. (1981) *J. Biol. Chem. 256*, 1377−1384.
Duquerroy, S., Camus, S., & Janin, J (1995) *Biochemistry 34*, 12513−12523.
Faller, L. D., & Johnson, A. M. (1974a) *Proc. Natl. Acad. Sci. U.S.A. 71*, 1083−1087.
Faller, L. D., & Johnson, A. M. (1974b) *FEBS Lett. 44*, 298−301.
Faller, L. D., Baroudy, B. M., Johnson, A. M., & Ewall, R. X. (1977) *Biochemistry 16*, 3864−3869.
Finzel, B. C. (1987) *J. Appl. Crystallogr. 20*, 53−55.
Hanlon, D. P., & Westhead, E. W. (1969) *Biochemistry 8*, 4247−4254.
Hendrickson, W. A., & Konnert, J. H. (1980) in *Biomolecular Structure, Function, Conformation and Evolution* (Srinivasan, R., Ed.) pp 43−57, Pregamon Press, Oxford.
Hilal, S. H., Carreira, L. H., & Karikhoff, S. W. (1994) in *Quantitative Treatment of Solute−Solvent Interactions* (Politzer, P., & Murray, V. S., Eds.) pp 291−353, Elsevier, Amsterdam.
Hilal, S. H., Brewer, J. M., Lebioda, L., & Carreira, L. A. (1995) *Biochem. Biophys. Res. Commun. 211*, 607−613.
Holleman, W. H. (1973) *Biochim. Biophys. Acta 327*, 176−185.
Jeffrey, G. A., & Saenger, W. (1991) *Hydrogen Bonding in Biological Molecules*, pp 15−37, Springer-Verlag, Berlin.
Kornblatt, M. J., & Musil, R. (1990) *Arch. Biochem. Biophys. 277*, 301−305.
Larsen, T. M., Wedekind, J. E., Rayment, I., & Reed, G. H. (1996) *Biochemistry 35*, 4349−4358.

Lebioda, L., & Stec, B. (1989) *J. Am. Chem. Soc. 111*, 8511−8513.
Lebioda, L., & Stec, B. (1991) *Biochemistry 30*, 2817−2822.
Lebioda, L., & Zhang, E. (1992) *J. Appl. Crystallogr. 25*, 323−324.
Lebioda, L., Stec, B., & Brewer, J. M. (1989) *J. Biol. Chem. 264*, 3685−3693.
Lebioda, L., Stec, B., Brewer, J. M., & Tykarska, E. (1991) *Biochemistry 30*, 2823−2827.
Lebioda, L., Zhang, E., & Brewer, J. M. (1996) *FASEB J. 10*, A1386.
Lee, M. E., & Nowak, T. (1992) *Arch. Biochem. Biophys. 293*, 264−273.
Lis, T. (1985) *Acta Crystallogr. C 41*, 1578−1580.
Navaza, J. (1987) *Acta Crystallogr. A 43*, 645−653.
Navaza, J. (1990) *Acta Crystallogr. A 46*, 619−620.
Nowak, T., Mildvan, A. S., & Kenyon, G. L. (1973) *Biochemistry 12*, 1690−1701.
Otwinowski, Z., & Minor, W. (1997) *Methods Enzymol. 276*, 307−326.
Poyner, R. R., Laughlin, L. T., Sowa, G. A., & Reed, G. H. (1996) *Biochemistry 35*, 1692−1699.
Reed, G. H., Poyner, R. R., Larsen, T. M., Wedekind, J. E., & Rayment, I. (1996) *Curr. Opin. Struct. Biol. 6*, 736−743.
Sangadala, V. S., Glover, C. V. C., Robson, R. L., Holland, M. J., Lebioda, L., & Brewer, J. M. (1995) *Biochim. Biophys. Acta 1251*, 23−31.
Shen, T. Y. S., & Westhead, E. W. (1973) *Biochemistry 12*, 3333−3337.
Stec, B., & Lebioda, L. (1990) *J. Mol. Biol. 211*, 235−248.
Stubbe, J. A., & Abeles, R. H. (1980) *Biochemistry 19*, 5505−5512.
Tulinsky, A., & Blevins, R. A. (1987) *J. Biol. Chem. 262*, 7737−7743.
Wedekind, J. E., Poyner, R. R., Reed, G. H., & Rayment, I. (1994) *Biochemistry 33*, 9333−9342.
Wedekind, J. E., Reed, G. H., & Rayment, I. (1995) *Biochemistry 34*, 4325−4330.
Westhead, E. W. (1966) *Methods Enzymol. 9*, 670−679.
Wold, F. (1971) in The *Enzymes* (Boyer, P. D., Ed.) Vol. 5, 3rd ed., pp 499−538, Academic Press, New York.
Wold, F., & Ballou, C. E. (1957) *J. Biol. Chem. 227*, 313−328.
Zhang, E., Lebioda, L., Chen, Y.-P., Brewer, J. M., Hatada, M., & Minor, W. (1994a) *Acta Crystallogr. D 50*, 335−336.
Zhang, E., Hatada, M., Brewer, J. M., & Lebioda, L. (1994b) *Biochemistry 33*, 6295−6300.

BI9712450